A new algorithm for transient motor current signature analysis using wavelets

H. Douglas
University of Cape Town
Department of Electrical Engineering
Rondebosch 7701
Cape Town, South Africa
hdougla@eng.uct.ac.za

P Pillay
Clarkson University
Department of Electrical and
Computer Engineering
Potsdam, NY, USA 13699-5720.E
pillayp@clarkson.edu

A K Ziarani
Clarkson University
Department of Electrical and
Computer Engineering
Potsdam, NY, USA 13699-5720.E
aziarani@clarkson.edu

***Abstract*— A new algorithm is introduced for motor current signature analysis of induction machines operating during transients. The algorithm is able to extract the amplitude, phase and frequency of a single sinusoid embedded in a non-stationary waveform. The algorithm is applied to the detection of broken rotor bars in induction machines during startup transients. The fundamental component of current, which varies in amplitude, phase and frequency, is extracted using the algorithm. The residual current is then analyzed using wavelets for the detection of broken rotor bars. This method of condition monitoring does not require parameters such as speed or number of rotor bars, is not load dependent and can be applied to motors that operate continuously in the transient mode e.g. wind generators or motor operated valves.**

***Keywords* - Condition Monitoring, Wavelets, Broken rotor bars.**

I. INTRODUCTION

THE induction machine is essential in many industrial applications. It is therefore desirable to reduce downtime by employing methods of machine condition monitoring. A widely used method of induction machine condition monitoring utilizes the steady-state spectral components of stator quantities. These spectral components can include voltage, current and power and can be used to detect broken rotor bars, bearing failures, air gap eccentricity etc. Traditionally these techniques have focused on the detection of faults during steady-state machine operation. [1-2]

The accuracy of these techniques depend on the loading of the machine, the assumption that the machine speed is constant, as well as the signal to noise ratio of the spectral components being examined.

The rotor bar frequencies are determined by

$$f_{rotorbar} = f_s\left[k\left(\frac{1-s}{p}\right)\pm s\right] \qquad (1)$$

where, k/p = 1,5,7,11,13…
f_s is the supply frequency
s is the machine slip
p is the number of poles.

These frequencies form the stator current spectrum shown in figure 1 and are present irrespective of the machine's condition. The presence of broken rotor bars is indicated by the difference in amplitude between the fundamental and the left sideband. A difference less than 50dB is an indication of broken rotor bars [3-7]. The amplitude of the left sideband frequency component of the fundamental frequency is proportional to the number of broken rotor bars present [8].

The right sideband component, $f_s(1+2s)$, could also be used in monitoring fault severity. Its importance is clearly demonstrated in [9-12].

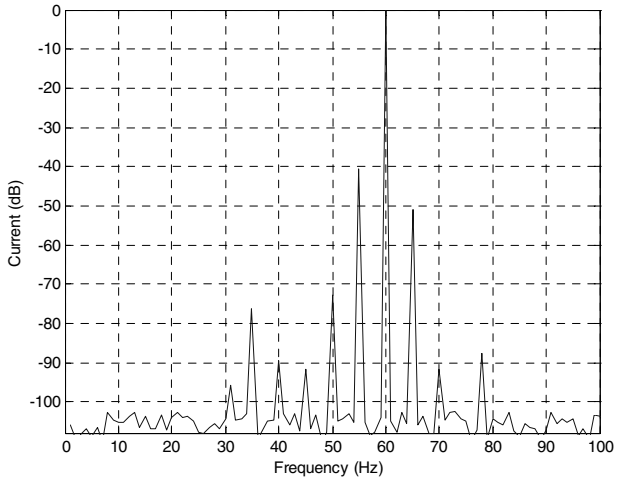

Fig. 1. A typical current spectrum of a fully loaded induction motor with broken rotor bars.

From (1) it is evident that the rotor bar frequencies are a function of the machine slip. If the machine is unloaded, the slip will be almost zero. The rotor bar frequencies will be masked by the fundamental frequency and thus make detection difficult. The only solution is therefore to heavily load the

machine in order to separate the frequencies. Overloading a machine is undesirable since it reduces the machine's operating lifetime and is not generally under control of the operator. Accurate detection therefore is difficult at light loading conditions. In addition many machines spend substantial periods at light loading conditions.

A fundamental disadvantage of the assumption of steady-state speed in condition monitoring is that there are many applications where constant speed operation is not achieved for example in wind generation or motor operated valves. In addition, the steady state algorithms focus only on low slips, while improved detection can be accomplished at high slips.

An alternate approach to the detection of broken rotor bars would be to examine the starting transient of an induction machine. The advantages would be that the transient has a high slip and high signal to noise ratio, which implies that the spectral components can be more easily separated. Loading does not affect the amplitude of the transient during startup. The load only affects the duration time of the startup transient. This implies that the detection can be done at low loading conditions unlike steady-state techniques.

A challenge of transient analysis is the difficulty in trying to analyze the complex transient startup current signal. This comprises a non-stationary fundamental frequency as well as non-stationary frequencies associated with the rotor bars. The rotor bar frequencies are a function of the machine speed slip and change as the machine runs up.

It is therefore desirable to be able to separate the fundamental frequency from the rotor bar frequencies. Using a high order notch filter will not accomplish this goal because the fundamental frequency is not constant.

A filter that actively tracks the changing amplitude, phase and frequency is needed to extract the fundamental from the transient. Once the fundamental frequency has been removed, the residual current can be examined using wavelets because the entire analysis is done in the transient [13-15] and is not amenable to study by Fourier Analysis.

II. DESCRIPTION OF THE ALGORITHM

Let $u(t)$ denote a signal comprising a sinusoidal component in addition to a number of additional components and noise. A sinusoidal component of this function, $y(t) = A\sin(\omega t+\delta)$, is of interest where A is the amplitude, ω is the frequency (in rad/s), δ is the phase and $\phi(t) = \omega t+\delta$ represents the total phase of this component. Ideally, parameters A, ω and δ are fixed quantities; but in practice, this assumption does not hold true.

Consider a general form of-

$$u(t) = u_0(t) + \sum_{i\neq 1} A_i sin(i\omega_0 + \delta_i).$$

Let M be a continuous manifold containing all sinusoidal signals defined as

$$M = \{y(t,\theta), t \in \Re, \theta_i \in \lfloor \theta^i{}_{,\min}, \theta^i{}_{,\max} \rfloor, i = 1,...,n, y : Sinusoid\}$$

where $\theta(t) = [\theta_1(t),...,\theta_n(t)]^T$ is the vector of parameters which belongs to the parameter space

$$\Theta = \{[\theta_1,...,\theta_n]^T \,|\, \theta_i \in [\theta^i{}_{\min}, \theta^i{}_{\max}], i = 1,...,n\},$$

and superscript T denotes matrix transposition.

The objective is to find an element in M which is closest to the sinusoidal component of the signal $u(t)$. The solution has to be an orthogonal projection of $u(t)$ onto manifold M, or equivalently it has to be an optimum θ which minimizes a distance function d between $y(t;\theta(t))$ and $u(t)$, i.e.,

$$\theta_{opt} = \arg \min_{\theta(t)\in\Theta} d[y(t,\theta(t)), u(t)].$$

The following instantaneous distance function d is used:

$$d(t,\theta(t)) = [u(t) - y(t,\theta(t))] = e(t).$$

Hence, the cost function is defined as $J(t,\theta(t)) = d^2(t, \theta(t))$. Although the cost function is not necessarily quadratic, the parameter vector θ is estimated using the gradient descent method-

$$\frac{d\theta(t)}{dt} = -\mu \frac{\partial[J(t,\theta(t))]}{\partial\theta(t)},$$

where the positive diagonal matrix μ is the algorithm regulating constant matrix. Given a quadratic cost function, it is clear that the algorithm employing this method converges to the minimum solution for the cost function. In more complex cases than those involving quadratic functions, the gradient descent method may still achieve minimization although this is not true in general. Global convergence of the gradient descent method is guaranteed for quadratic distance functions; otherwise, its convergence has to be directly proven.

The output signal is defined as-

$$y(t) = A(t)\sin(\int^t \omega(\tau)d\tau + \delta(t)).$$

Formulating the algorithm accordingly using the parameter vector $\theta = [A,\delta,\omega]$, i.e. the amplitude, phase angle and frequency of the desired component, results in the following set of equations[1]:-

$$\dot{A}(t) = \mu_1 e(t) sin\phi(t), \qquad (2)$$

$$\dot{\omega}(t) = \mu_2 e(t) A(t) cos\phi(t), \qquad (3)$$

$$\dot{\phi}(t) = \mu_1\mu_2 e(t) A(t) cos\phi(t) + \omega(t), \qquad (4)$$

[1] Strictly following the least squares error minimization using the method of gradient descent results in a time-varying set of equations in which the time variable t is explicitly present in the equations. In the equations presented here, the time variable t is replaced by a constant number. This replacement converts the time-varying system into a time-invariant system. The apparently arbitrary formulation of the algorithm calls for mathematically rigorous justification which is presented in [16-17].

$$y(t) = A(t)\sin\phi(t), \quad (5)$$

$$e(t) = u(t) - y(t). \quad (6)$$

The dot on top ($\dot{}$) represents the differentiation with respect to time. Note that $\dot{\phi} = \omega + \dot{\delta}$ is used in deriving the third differential equation. State variables $A(t)$, $\phi(t)$ and $\omega(t)$ directly provide instantaneous estimates of the amplitude, phase and frequency of the extracted sinusoid, respectively. Undesired components and noise imposed on the sinusoidal component of interest altogether are provided by *e(t)*. The parameters μ_1, μ_2 and μ_3 are positive numbers which determine the behavior of the algorithm in terms of convergence rate versus accuracy. This dynamic model presents an algorithm which is capable of extracting a specified sinusoidal signal, estimating its amplitude, frequency and phase, and accommodating variations in the amplitude, frequency and phase of such a sinusoidal component.

Equations (2) to (6) constitute the governing set of equations of the generalized algorithm. The following theorem, proved in [17], deals with the stability issues of this dynamical system:

Theorem 1: Let $u(t) = A_o \sin(\omega_o t + \delta_o) + g(t)$ where A_o, ω_o, and δ_o are real constants and $g(t)$ is an arbitrary T_o–periodic bounded continuous function which has no frequency component at ω_o. For a proper choice of parameters $\{\mu_i, i = 1, 2,3\}$, the dynamical system (2) to (6) has a unique periodic orbit $\gamma(t)$ in (A, ω, ϕ) space in a neighborhood of $u_o(t)=A_o\sin(\omega_o t + \delta_o)$. This neighborhood is determined by the function $g(t)$ and the parameters μ_1 to μ_3. Moreover, this periodic orbit is asymptotically stable. The periodic orbit coincides with $u_o(t)$ when $g(t)$ is zero.

The theorem indicates that there is a unique periodic orbit to which the system converges. This periodic orbit is located in a neighborhood of the ideal desired component. The tighter this neighborhood is, the more accurately the desired component is estimated. The extent of this neighborhood is determined by the level of "pollution" $g(t)$ and the step sizes μ_1, μ_2 and μ_3. Smaller values for step sizes μ_1 and μ_2 result in a more refined periodic orbit in a tighter neighborhood. On the other hand, the step-sizes determine the speed of the convergence to the solution of the differential equations. As well, if the parameters in the input function (including amplitude and phase angle) vary with time, the desired solution will follow those variations provided that the speed of the convergence to the solution, determined by the step sizes, is sufficiently high. A trade-off. therefore exists between the transient convergence speed and the steady state accuracy.

In terms of the engineering performance of the system, this indicates that the output of the system will approach a sinusoidal component of the input signal $u(t)$. Moreover, time variations of parameters in $u(t)$ are tolerated by the system.

Figure 2 shows a snapshot of the performance of the algorithm when the frequency and amplitude of the input signal jump from 50 Hz to 100 Hz and 1 to 2, respectively. Initially, the periodic orbit is a circle with unit radius which lies on the horizontal plane of f = 50 Hz, then it flows to another circle with radius 2 which lies on the plane of f = 100Hz.

Figure 3 shows implementation of the algorithm in the form of composition of simple blocks suitable for schematic software development tools. Numerically, a possible way of writing the set of equations governing the present algorithm in discrete form, which can be readily used in any programming language, is

$$A[n+1] = A[n] + T_s\mu_1 e[n]\sin\phi[n], \quad (7)$$

$$\omega[n+1] = \omega[n] + T_s\mu_2 e[n]A[n]\cos\phi[n], \quad (8)$$

$$\phi[n+1] = \phi[n] + T_s\omega[n] + T_s\mu_2\mu_3 e[n]A[n]\cos\phi[n], \quad (9)$$

$$y[n] = A[n]\sin\phi[n], \quad (10)$$

$$e[n] = u[n] - y[n]. \quad (11)$$

where a first order approximation for derivatives is assumed; in other words, the time-derivative of a quantity X is approximated by $\frac{X[n+1]-X[n]}{T_s}$ in discrete form. The iterative expression of (8) is used to provide the value of frequency ω needed in (4) which results in the explicit expression of (9). *Ts* is the sampling time and *n* is the time index.

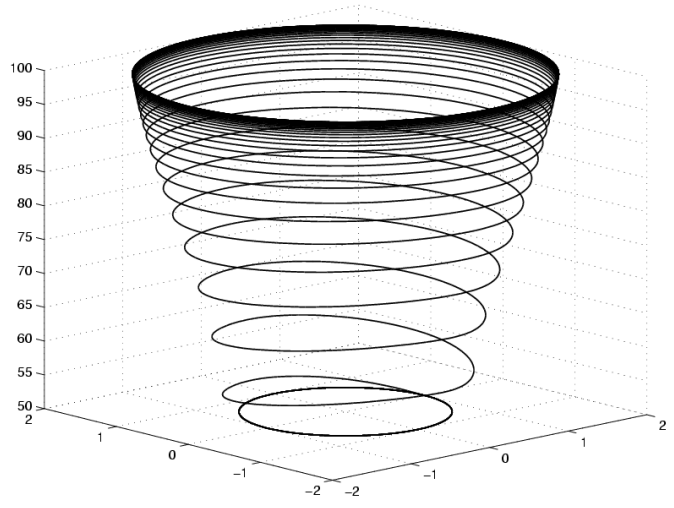

Fig. 2. Phase portrait diagram when both the amplitude and frequency of the input signal undergo a jump of 100%.

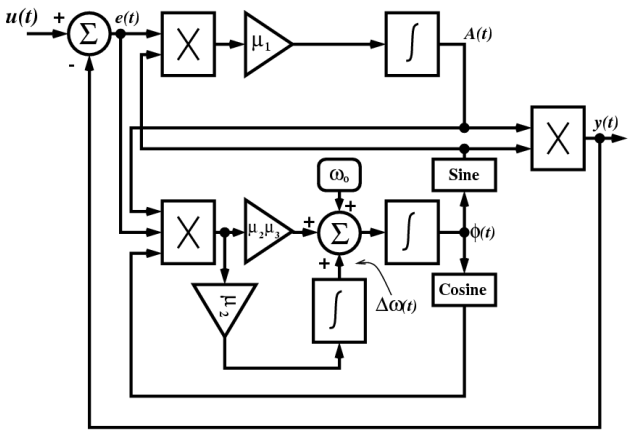

Fig. 3. Block Diagram implementation of the algorithm.

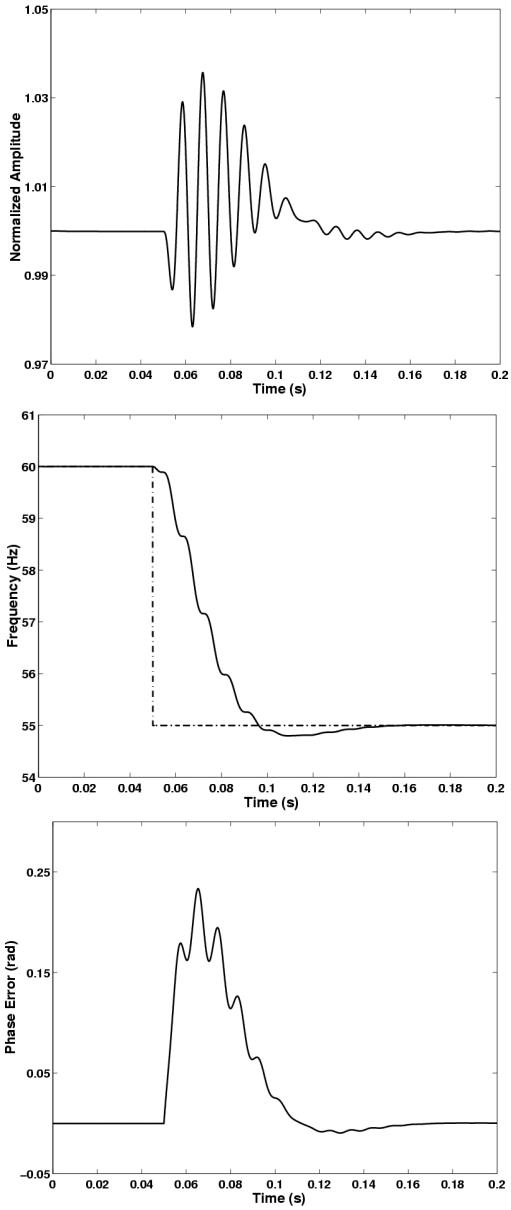

Fig. 4. Response of the algorithm to a step change in the frequency of the input signal.

In the simulations presented in this paper, Matlab Simulink™ computational software is used as the main computational tool. Figure 4 shows the performance of the algorithm for an example in which the frequency of the input signal undergoes a step change of 10%. It is observed that the variations are effectively tracked with a transient lasting just a few cycles. Values of the parameters are chosen to be μ_1 = 100, μ_2 = 10000 and μ_3 = 0.02 for this simulation.

The dynamics of the algorithm presents a notch filter in the sense that it extracts (i.e. lets pass through) one specific sinusoidal component and rejects all other components including noise. It is adaptive in the sense that the notch filter accommodates variations of the characteristics of the desired output over time. The center frequency of such an adaptive notch filter is specified by the initial condition of frequency ω. In Figure 3 this initial value, ω_o, is explicitly shown for easy visualization.

III. APPLICATION OF THE ALGORITHM

The measured startup current transient of an 11kW induction motor is shown in Figure 5. Before implementing the algorithm, the individual measured line currents are transformed into a single rotating current vector as shown in Figure 6. This vector is then transformed into the time domain and used as an input to the extraction algorithm. The algorithm estimates the frequency, amplitude and phase of the nonstationary fundamental as shown in Figures 7,8,9. The fundamental component (which varies with magnitude, frequency and phase) can be extracted with this algorithm. This estimate is then subtracted from the input. The resulting waveform shown in Figure 10 has information relating to the health of the machine including bad bearings, broken rotor bars etc.

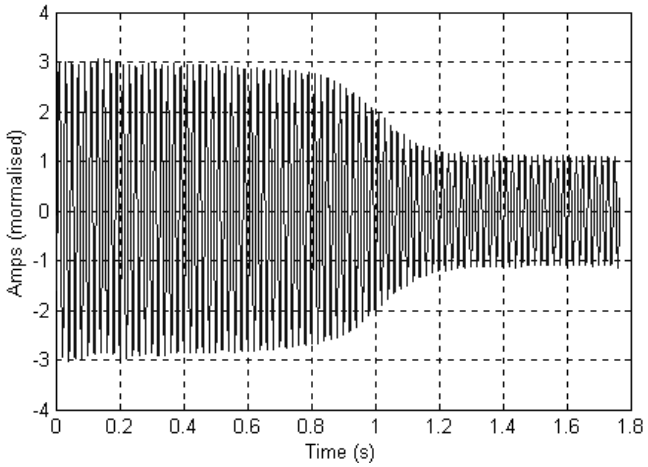

Fig. 5. Startup current transient.

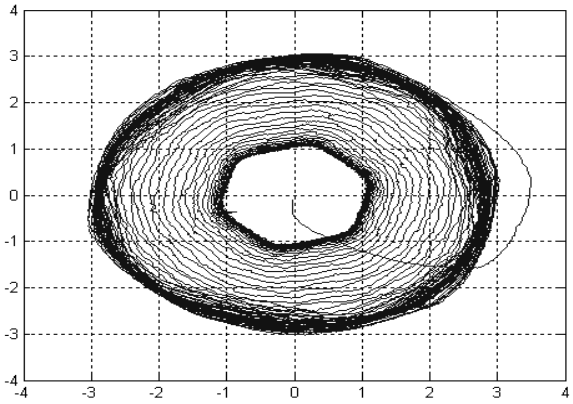

Fig. 6. A plot of the current vector.

The algorithm takes a few cycles to converge to the amplitude and frequency of the fundamental. This is shown in Figures 8 and 10. As a result when the estimated fundamental is subtracted from the original waveform, the algorithm's output between 0 and 0.4 seconds should be discarded to allow for convergence.

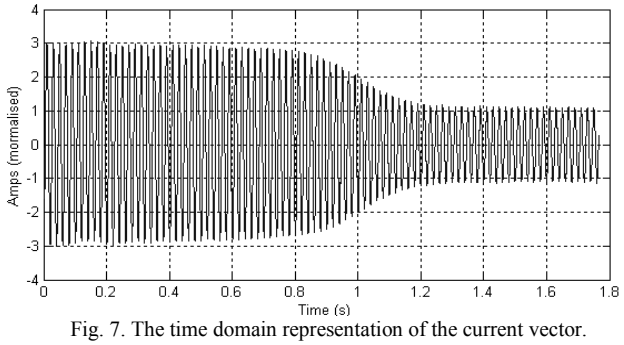

Fig. 7. The time domain representation of the current vector.

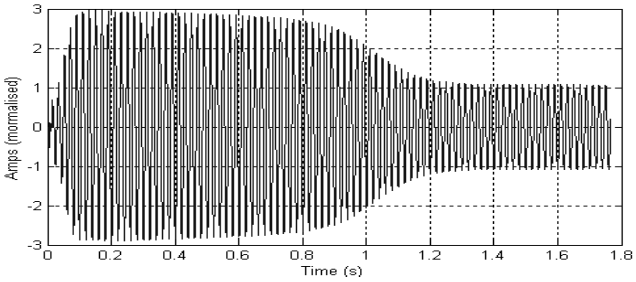

Fig. 8. The estimated fundamental startup current of the algorithm.

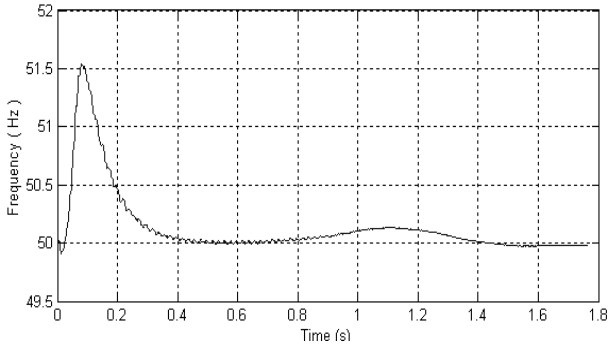

Fig. 9. Frequency of the algorithm.

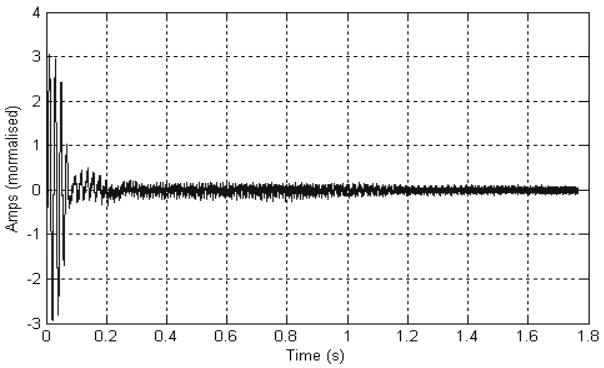

Fig 10. The startup current after extraction of the fundamental.

Figure 10 shows the estimated frequency of the fundamental. An accurate estimate of the frequency is only available after 0.4s.

IV. DETECTION OF BROKEN ROTOR BARS

The algorithm was used to detect broken rotor bars in a ½ hp induction motor. Two identical rotors were used in this experiment except that one had a broken rotor bar. The same bearings and stator was used in order to minimize their influences on the startup transients. The machine was tested under loading conditions varying from 30% to 100% to determine if this method of detection could be successful and independent of the loading conditions.

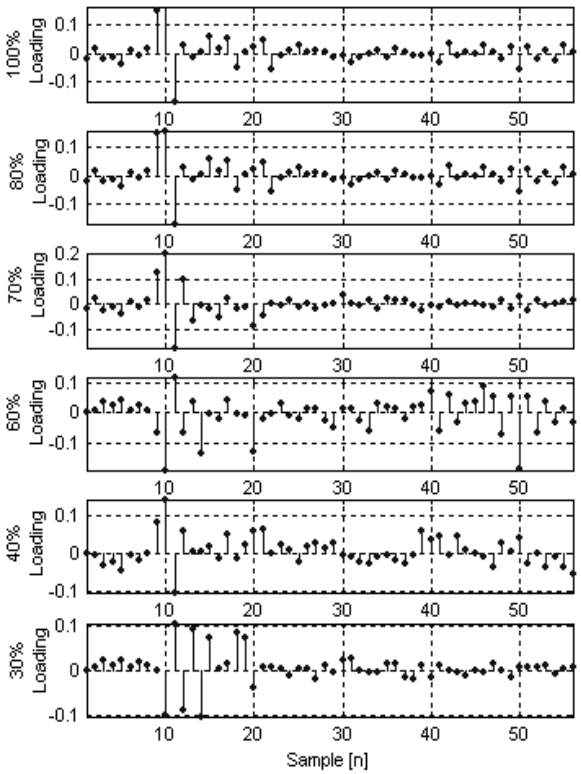

Fig. 11. Wavelet decomposition levels D9 of a healthy machine loaded 30% to 100%.

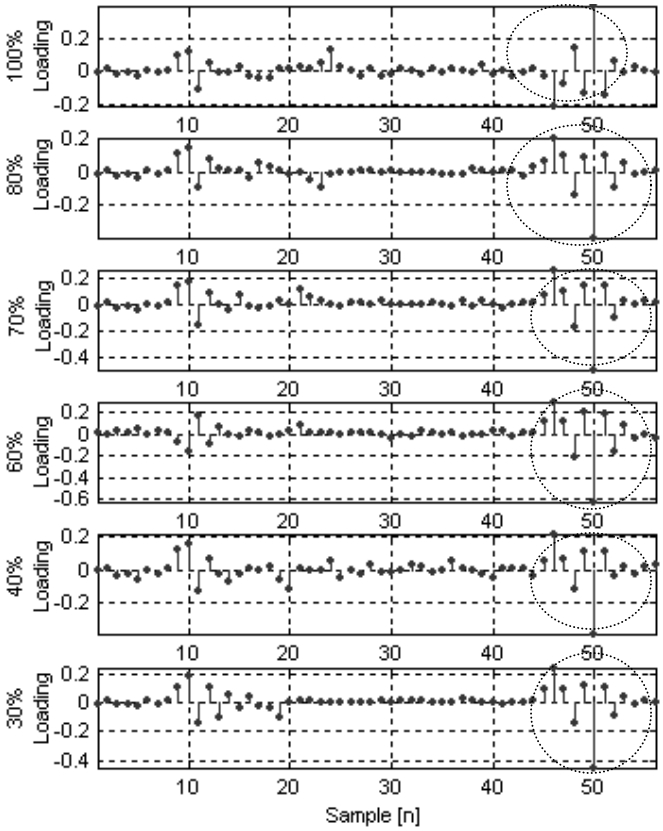

Fig. 12. Wavelet decomposition levels D9 of a damaged machine loaded 30% to 100%.

The fundamental frequency of the stator current vector was removed from the total inrush current using the extraction algorithm. The discrete wavelet transform, using Daubechies 8 wavelet, was then applied to the residual current vector. Figures 11 and 12 show the level 9 detail coefficients of both healthy and damaged machine under various loads. By inspection of figures 11 and 12, two dominant features are present that characterize the condition of the machine. The first feature is found between samples 8 and 13 of all the loading conditions. This feature is present in both the healthy and damaged machine. The second feature found between samples 45 and 53 is only present in the case of the damaged machine. The second feature can be used to discriminate between a healthy and a damaged machine. An automated fault detection analyzer is envisioned based on this algorithm.

V. CONCLUSIONS

A new algorithm for use in transient motor current signature analysis has been introduced and applied to the detection of broken rotor bars in induction machines. The algorithm is able to extract a single non-stationary sinusoid embedded within a non-stationary waveform.

This is then applied to the transient inrush current of an induction motor and a wavelet analysis is conducted on the balance of the current.

Although results presented here are unique to the machine being diagnosed, the methodology applied to extracting the transient fundamental current and analysis of the residual currents is universal and can be applied to any machine.

The analysis clearly shows that the broken rotor bar can be can be detected using measured transient inrush currents. This method can be used for standard induction motors during startups as well as machines that operate predominantly in the transient like wind generators or motor operated valves.

ACKNOWLEDGMENTS

The authors acknowledge the University of Cape Town Power Engineering Group for assistance with this project and the US Navy ONR for financial assistance.

REFERENCES

[1] G. B. Kliman *et al.*, "Methods of motor current signature analysis,"*Elect. Mach. Power Syst.*, vol. 20, no. 5, pp. 463–474, Sept. 1992.

[2] W. Deleroi, "Broken bars in squirrel cage rotor of an induction motor—Part1: Description by superimposed fault currents", *Arch. Elektrotech.*, vol. 67, pp. 91–99, 1984.

[3] R. Hirvonen, "On-line condition monitoring of defects in squirrel cage motors," in *Proc. 1994 Int. Conf. Electrical Machines*, vol. 2, Paris.

[4] Benbouzid & M. Vieira, "Induction Motor Fault Detection and Localization Using Stator Current, Advanced Signal Processing Technique*". IEEE Trans. Industrial Application 1995, Vol. 3, No. 1*

[5] S. L. Ho, W. L. Chan and H. W. Leung, "Application of Statistical Signal Processing for Condition Monitoring of Rotor Faults in Induction Motor". *Electrical Machines and Drives, Sixth International Conference* PP. 97 – 102, 1993.

[6] G. B. Kliman, J. Stein, "Induction Motor Fault Detection Via Passive Current Monitoring a Brief Survey." PP. 49-65

[7] W. T. Thomson, I. D. Stewart, "On-line Current Monitoring for Fault Diagnosis in Inverter Fed Induction Motor". Life Management of Power Plants, 1994., International Conference, PP. 66 – 73.

[8] C. Hargis *et al.*, "The detection of rotor defects in nduction motors," in *Proc. 1982 IEE Int. Conf. Electrical Machines, Design and Application*, London, U.K., pp. 216–220.

[9] Mohamed El Hachemi Benbouzid," A Review of Induction Motors Signature Analysis as a Medium for Faults Detection *"IEEE Transactions on Industrial Electronics,* VOL. 47, NO. 5, October 2000

[10] W. Deleroi" Squirrel Cage Motor with Broken Bar in the Rotor- Physical Phenomena and their Experimental Assessment", Proc. ICEM'82. Budapest, Hungary, 1982, pp. 767-770.

[11] H. A. Toliyat *et al.*, "Condition monitoring and fault diagnosis of electrical machines—A review," in *Conf. Rec. 1999 IEEE-IAS Annual. Meeting*, vol. 1, Phoenix, AZ, pp. 197–204.

[12] F. Filippetti *et al.*, "AI techniques in induction machines diagnosis including the speed ripple effect," *IEEE Trans. Ind. Applicat.*, vol. 34, pp. 98–108, Jan./Feb. 1998.

[13] O. Rioul and M. Vettrli, "Wavelet and Signal Processing" *IEEE SP Magazine*, October 1991, PP.14-38

[14] S. G. Mallat, "A Wavelet Tour of Signal Processing", Academic Press, 1998.

[15] M. Haji, H. A. Toliyat, "Pattern Recognition – A Technique for Induction Machines Rotor Fault Detections," *Proceedings of the IEEE IEMDC'* 01, Boston, MA, June 17-20, 2001.

[16] Ziarani, A.K.; Konrad, A." A nonlinear adaptive method of elimination of power line interference in ECG signals" *"IEEE Transactions on Biomedical Engineering,* Volume: 49, Issue: 6, June 2002

[17] M. Karimi-Ghartemani and A. K. Ziarani, "Periodic orbit analysis of two dynamical systems for electrical engineering applications," *Journal of Engineering Mathematics*, Vol. 45, No. 2,2003, pp. 135-154.

[18] P.Pillay and Z.Xu, "Motor Current Signature Analysis", *IEEE IAS Annual* Meeting, Oct 1996.